Photoelastic and acousto-optical properties of Cs_2HgCl_4 crystals

Mykola V. Kaidan, Anna V. Zadorozhna, Anatolij S. Andrushchak, and Andriy V. Kityk

We use a Mach–Zehdner interferometric technique to study the piezo-optical properties of Cs_2HgCl_4 crystals at room temperature. All piezo-optical (π_{mn}) and photoelastic (p_{in}) tensor constants are obtained. A substantial photoelastic effect and low ultrasonic velocities in these crystals determine a relatively high figure of merit M_2 for isotropic diffraction (for a certain geometry of acousto-optical interactions, $M_2 \sim 110 \times 10^{-15}$ s^3/kg). The new material may be considered, therefore, a candidate for applications in acousto-optical devices. The dependence of the acoustic walk-off angle on the direction of sound propagation is calculated for the principal crystallographic planes.

OCIS codes: 160.1050, 160.4760.

1. Introduction

Cesium mercury tetrachlorate (Cs_2HgCl_4) is a member of a large family of insulating crystals with the general formula A_2BX_4 (A = K, Rb, Cs, NH_4 . . . ; B = Zn, Mn, Co, Hg, Fe . . . ; X = Cl, Br, J). According to the results of x-ray diffraction[1] the normal paraelastic phase in these crystals appears above $T_i \approx 221$ K. It has a β-K_2SO_4-type structure with orthorhombic space group $Pnma$ and four formula units per unit cell. Results of dielectric, calorimetric, and Raman investigations indicate a series of structural transformations, including the normal incommensurate phase transition at $T = T_i$, and several other transitions associated with ferroelastic or ferroelectric instabilities that occur in the temperature region below T_i.[2–4] Optical birefringence and acoustic methods were used for a detailed pressure–temperature phase diagram of Cs_2HgCl_4.[5–7] All components of the elastic constant (C_{ij}) and the elastic compliance (S_{ij}) tensors in a wide temperature range were determined.[7]

In spite of numerous investigations, the photoelastic properties of Cs_2HgCl_4 crystals have not to our knowledge been studied. At the same time, they can be considered new perspective materials for acousto-optical applications: a substantial figure of merit M_2 is expected here because of the low magnitudes of the ultrasonic velocities.[7] In addition, a wide spectral range of crystal transparency (310–15,000 nm; Ref. 8) appears to be important in modern laser technology and optical information processing for control of the parameters of optical beams. Hence our purposes in this paper are to report detailed piezo-optical investigations and to estimate the efficiency of isotropic and anisotropic acousto-optical diffraction in this material.

2. Experimental Procedure and Results

The piezo-optical measurements were performed at room temperature with a He–Ne laser (λ = 632.8 nm). The experimental setup for these measurements was a Mach–Zehnder interferometric technique.[9,10] Such a procedure yields a possibility of determining both the magnitude and the sign of piezo-optical constants π_{im}, which makes it superior to conventional acousto-optical methods from which only the absolute values of photoelastic constants p_{in} can be obtained.[11] A slightly modified setup was suitable for simultaneous interferometric and optical-polarization measurements. We measured the changes induced in the optical path, $\delta\Delta_{ikm}$, and the induced retardation, $\delta\Delta_{km}{}^{o}$, to obtain both the conventional piezo-optical constants π_{im} and the effective piezo-optical constants of induced birefringence $\pi_{km}{}^{*} = \pi_{im}n_i{}^3 - \pi_{jm}n_j{}^3$ with no change in sample position. We used simultaneous estimations

M. V. Kaidan, A. V. Zadorozhwa, and A. S. Andrushchak are with the Institute of Physical Optics, Dragomanov Str. 23, 79005, L'viv, Ukraine. A. V. Kityk (kityk@ap.univie.ac.at) is with the Institute for Computer Science, Department of Electrical Engineering, Technical University of Czestochowa, Al. Armii Krajowej 17, PL-42200, Czestochowa, Poland.

Received 30 November 2001; revised manuscript received 21 March 2002.

0003-6935/02/255341-05$15.00/0

of these constants to test the validity of the experimental data. The piezo-optical constants π_{im} and $\pi_{km}{}^{*}$ were calculated from the following expressions:

$$\pi_{im} = -\frac{2\delta\Delta_{ikm}}{\sigma_m t_k n_i{}^3} + \frac{2S_{km}(n_i - 1)}{n_i{}^3}$$

$$(i, m = 1, 2, 3), \tag{1}$$

$$\pi_{rr} = -4n_r{}^{-3}\left(\frac{\delta\Delta_{r\bar{r}r}}{t_{\bar{r}}\sigma_r} - \frac{\delta\Delta_{\bar{r}r\bar{r}}}{t_r\sigma_{\bar{r}}}\right) + n_r{}^{-3}(n_r - 1)(S_{ii} + S_{jj} + 2S_{ij} - S_{rr}) - (\pi_{ii} + \pi_{ij} + \pi_{ji} + \pi_{jj})/2$$

$$[r = 9 - i - j = 4, 5, 6, \quad i \neq j = 1, 2, 3, \quad n_r = \sqrt{2}n_i n_j(n_i{}^2 + n_j{}^2)^{-1/2}], \tag{2}$$

$$\pi_{km}{}^{*} = -\frac{2\delta(\Delta n_k)}{\sigma_m} = \frac{2\delta\Delta_{km}{}^{o}}{\sigma_m} + 2\Delta n_k S_{km} = \pi_{km}{}^{o} + 2\Delta n_k S_{km}, \tag{3}$$

where σ_m is the mechanical stress, n_i and n_j are the principal refractive indices, t_k and t_r are the sample thicknesses along the direction of light propagation; S_{km} is the elastic (see the definition below) compliance, $\Delta n_k = n_i - n_j$ is the optical birefringence, $\delta(\Delta n_k)$ is the induced birefringence, and $\pi_{km}{}^{o} = 2\delta\Delta_{km}{}^{o}/\sigma_m$ is the constant of the induced retardation; 4, 5, and 6 are the diagonal directions between the principal crystallographic axes (Y, Z), (X, Z), and (X, y), respectively. As follows from Eqs. (1) and (3), the piezo-optical effect is presented here by two terms, which correspond to direct (photoelastic) and to nondirect (elastic) contributions. The sign of the induced value $\delta\Delta_{ikm}$ ($\delta\Delta_{km}{}^{o}$) and, therefore, the signal of the piezo-optical constant π_{im} ($\pi_{km}{}^{*}$) was determined by use of the criteria described in Ref. 9.

Single crystals of Cs_2HgCl_4 were grown from the melt by the Bridgman method. We used the following crystallographic orientation: $c > a > b$ ($c \approx \sqrt{3}b$), where a is the pseudohexagonal axis.[1] The piezo-optical and photoelastic constants are usually related to an orthonormal set of axes $X = 1$, $Y = 2$, and $Z = 3$, which, for the orthorhombic structure, possess a standard orientation with respect to the principal crystallographic axes: $a \equiv X$, $b \equiv Y$, and $c \equiv Z$.

The measurements of the piezo-optical constants $\pi_{im} = \pi_{qlrs}$ ($i \equiv ql$, $m \equiv rs$; $i, m = 1, \ldots, 6$; $1 \equiv 11$, $2 \equiv 22$, $3 \equiv 33$, $4 \equiv 23 \equiv 32$, $5 \equiv 13 \equiv 31$, $1 \equiv 12 \equiv 21$) were made either of rectangular samples oriented along the principal crystallographic directions (direct-cut samples for $i, m = 1, 2, 3$) or on the $X/45°$-$Y/45°$- and $Z/45°$-cut samples prepared again in a rectangular form (for $i = m = 4$–6). The samples were typically approximately 5 mm × 5 mm × 5 mm in size. Piezo-optical measurements were made of electrically unshorted samples, i.e., at a constant electric displacement. The refractive indices of Cs_2HgCl_4 were measured by Obreimov's immersion method, which gives the following values for the principal refractive indices ($\lambda = 632.8$ nm; Ref. 8): $n_1 = 1.6498$, $n_2 = 1.6690$, and $n_3 = 1.6491$.

The results of the piezo-optical measurements of Cs_2HgCl_4 crystals are presented in Tables 1 and 2. The following values of the elastic compliances were used for the calculations: $S_{11} = 62.86$, $S_{22} = 104.6$, $S_{33} = 100.2$, $S_{12} = -28.56$, $S_{13} = -28.85$, $S_{23} = -32.66$, $S_{44} = 325.7$, $S_{55} = 220.3$, and $S_{66} = 327.9$ [all numbers are Brewster units (Br): 1 Br = 10^{-12} m^2/N) (Ref. 7)]. The measured constants are presented here, together with their absolute errors that we have evaluated, taking into account the applied load error (the relative error is ~5%), the error in registration of an interference pattern shift (~0.02 of the interference fringe width), and the error in the elastic compliances (the last digit is assumed to be significant). The errors in crystal length and in refractive index were neglected, as we consider their magnitudes to be infinitesimal.

Table 1 contains the data as obtained by interferometric and optical-polarization methods. The samples have been compressed along the principal crystallographic directions [100], [010], and [001] and obviously produce only the deformation of an optical indicatrix. The data presented in the Table 1 [i.e., the effective driving half-wave stress $\sigma_{km}{}^{o} = \sigma_{km}{}^{\lambda/2}t_k$, the piezo-optical constants π_{im} and $\pi_{km}{}^{*}$, and the fraction of the direct (pure photoelastic)/nondirect (elastic) contribution to $\delta\Delta_{ikm}$ ($\delta\Delta_{km}{}^{o}$)] obviously form a complete characterization of the piezo-optical properties of Cs_2HgCl_4 crystals. A comparison of the data obtained for various sample geometries proves their validity. We point out some facts here:

(i) The values of piezo-optical constants π_{22} and π_{33} obtained at different sample geometries coincide within the experimental errors. This fact testifies to the satisfactory precision in our experiments.

(ii) The photoelastic and elastic contributions to $\delta\Delta_{ikm}$ were comparable when stress was applied along the Y or the Z axis. Both contributions have the same sign. The elastic contribution if significantly larger than photoelastic contribution for compression applied along the X axis. Driving half-wave stress $\sigma_{km}{}^{o}$ is the largest in this case.

(iii) Piezo-optical constants $\pi_{km}{}^{*}$ measured directly by the optical-polarization technique coincide within the experimental errors with the values $\pi_{km}{}^{*}$ that have been calculated by use of piezo-optical constants π_{im} measured by the interferometric method. The photoelastic contribution to the induced retardation, $\delta\Delta_{km}{}^{o}$, is sufficiently larger than the elastic contribution.

Table 2 contains the data as obtained by interferometric and optical-polarization techniques with $X/45°$, $Y/45°$, and $Z/45°$ cuts of Cs_2HgCl_4 crystals. Compression was applied along the [110], [101], and [011] directions, which caused rotation of the optical indicatrices in the XY, XZ, and YZ planes, respectively. The values of the nonprincipal diagonal piezo-optical constants π_{44}, π_{55}, an π_{66} were calcu-

Table 1. Piezo-Optical Effect in Cs_2HgCl_4 Crystals[a]

Interferometric Measurements: Sample Geometry k	m	i	Driving Effective Stress σ°_{km}[b] (N/m × 10^3)	Piezo-optical Constant π_{im} (Br)	Direct (Photoelastic) Contribution to $\delta\Delta_{ikm}$ (%)	Nondirect (Elastic) Contribution to $\delta\Delta_{ikm}$ (%)	Effective Piezo-Optical Constants $\pi_{km}{}^*$ Calculated from π_{im} (Br)	Optical Polarization Measurements: Driving Effective Stress $\sigma_{km}{}^{\circ}$ (N/m × 10^3)[b]	Direct (Piezo-Optical) Contribution to $\pi_{km}{}^*$ (Br)	Nondirect (Elastic) Contribution $\pi_{km}{}^*$ (Br)	Piezo-optical constants $\pi_{km}{}^*$ (Br)
2	3	1	−5.8	$\pi_{13} = 14.8 \pm 0.9$	61	39	$\pi_{23}{}^* = \pi_{33}{n_3}^3$	−109	−5.8 (100%)	<0.05 (~0%)	$\pi_{23}{}^* = -5.8 \pm 0.24$
2	3	3	−6.0	$\pi_{33} = 13.9 \pm 0.9$	60	40	$-\pi_{13}{n_1}^3 = -4.2$				
1	3	2	−5.8	$\pi_{23} = 16.6 \pm 0.9$	67	33	$\pi_{13}{}^* = \pi_{23}{n_2}^3$	−27.3	23.6 (105%)	−1.2 (−5%)	$\pi_{13}{}^* = 22.4 \pm 0.9$
1	3	3	−6.9	$\pi_{33} = 12.6 \pm 0.8$	60	40	$-\pi_{33}{n_3}^3 = 21.2$				
3	2	1	−5.2	$\pi_{12} = 17.5 \pm 0.9$	65	35	$\pi_{32}{}^* = \pi_{12}{n_1}^3$	−29.3	21.6 (94%)	1.3 (6%)	$\pi_{32}{}^* = 22.9 \pm 0.9$
3	2	2	−6.5	$\pi_{22} = 12.3 \pm 0.8$	57	43	$-\pi_{22}{n_2}^3 = 21.4$				
1	2	3	−9.1	$\pi_{32} = 7.3 \pm 0.6$	47	53	$\pi_{12}{}^* = \pi_{22}{n_2}^3$	−31.7	20.0 (106%)	−1.1 (−6%)	$\pi_{12}{}^* = 18.9 \pm 0.8$
1	2	2	−7.0	$\pi_{22} = 11.3 \pm 0.8$	58	42	$-\pi_{32}{n_3}^3 = 19.9$				
3	1	2	−20	$\pi_{21} = -1.4 \pm 0.3$	−20	120	$\pi_{31}{}^* = \pi_{11}{n_1}^3$	−29.9	21.2 (95%)	1.2 (5%)	$\pi_{31}{}^* = 22.4 \pm 0.9$
3	1	1	−12	$\pi_{11} = 3.2 \pm 0.5$	28	72	$-\pi_{21}{n_2}^3 = 20.8$				
2	1	3	−22	$\pi_{31} = -1.7 \pm 0.3$	−26	126	$\pi_{21}{}^* = \pi_{31}{n_3}^3$	−52	−12.2 (100%)	<0.05 (~0%)	$\pi_{21}{}^* = -12.2 \pm 0.5$
2	1	1	−14	$\pi_{11} = 1.5 \pm 0.4$	15	85	$-\pi_{11}{n_1}^3 = -14.4$				

[a]The mechanical compression is parallel to the principal crystallographic direction.
[b]Driving effective half-wave mechanical stress: $\sigma_{km}{}^{\circ} = \sigma_m{}^{\lambda/2} t_k$, where $\sigma_m{}^{\lambda/2}$ is half-wave mechanical stress, t_k is the thickness of the sample along the direction of light propagation, **k** is the direction of light propagation, **m** is the direction of sample compression, and **i** is the direction of light polarization.

Table 2. Piezo-Optical Effect in Cs_2HgCl_4 Crystals Measured on *X*/45°-, *Y*/45°-, and *Z*/45°-Cut Samples[a]

	Sample Geometry k	m	i	Measured Effectve Piezo-optical Constant	Values Calculated from Interferometric Measurements: Piezo-Optical Constant: One-Stage Measurement Method	Two-Stage Measurement Method	Effective Piezo-optical Constant $\pi_{km}{}^*$	Optical-Polarization Measurement $\pi_{km}{}^*$
1	4	$\bar{4}$	1	$\pi_{1\bar{4}}{}' = (\pi_{12} + \pi_{13})/2 = 11.6 + 0.6 \quad (16.7)^b$	$\pi_{44} = -10.8 \pm 1.3$	$\pi_{44} = -11.0 \pm 1.9$	$\pi_{\bar{4}\bar{4}}{}^* = \pi_{\bar{4}\bar{4}}{}'{n_4}^3 - \pi_{1\bar{4}}{}'{n_1}^3 = -21$	$\pi_{\bar{4}\bar{4}}{}^* = -29 \pm 1$
	4	$\bar{4}$	$\bar{4}$	$\pi_{\bar{4}\bar{4}}{}' = (\pi_{22} + \pi_{23} + \pi_{32} + \pi_{33} + 2\pi_{44})/4 = 6.8 \pm 0.5$				
1a	$\bar{4}$	4	1	$\pi_{14}{}' \equiv \pi_{1\bar{4}}{}' = 14.8 \pm 0.8 \quad (16.7)^b$	$\pi_{44} = -11.3 \pm 1.1$	$\pi_{44} = -11.0 \pm 1.9$	$\pi_{\bar{4}\bar{4}}{}^* = \pi_{44}{}'{n_4}^3 - \pi_{14}{}'{n_1}^3 = -36$	$\pi_{\bar{4}\bar{4}}{}^* = -31 \pm 1$
	$\bar{4}$	4	4	$\pi_{44}{}' \equiv \pi_{\bar{4}\bar{4}}{}' = 6.6 \pm 0.4$				
2	5	$\bar{5}$	2	$\pi_{2\bar{5}}{}' = (\pi_{21} + \pi_{23})/2 = 6.0 \pm 0.5 \quad (7.6)^b$	$\pi_{55} = -5.3 \pm 0.8$	$\pi_{55} = -5.8 \pm 1.1$	$\pi_{5\bar{5}}{}^* = \pi_{2\bar{5}}{}'{n_2}^3 - \pi_{\bar{5}\bar{5}}{}'{n_5}^3 = 7.5$	$\pi_{5\bar{5}}{}^* = 8.3 \pm 0.3$
	5	$\bar{5}$	$\bar{5}$	$\pi_{\bar{5}\bar{5}}{}' = (\pi_{31} + \pi_{33} + \pi_{11} + \pi_{13} + 2\pi_{5\bar{5}})/4 = 4.5 \pm 0.3$				
2a	$\bar{5}$	5	2	$\pi_{25}{}' \equiv \pi_{2\bar{5}}{}' = 5.2 \pm 0.4 \quad (7.6)^b$	$\pi_{55} = -6.4 \pm 0.8$	$\pi_{55} = -5.8 \pm 1.1$	$\pi_{\bar{5}\bar{5}}{}^* = \pi_{25}{}'{n_2}^3 - \pi_{55}{}'{n_5}^3 = 4.3$	$\pi_{\bar{5}\bar{5}}{}^* = 3.3 \pm 0.2$
	$\bar{5}$	5	5	$\pi_{55}{}' \equiv \pi_{\bar{5}\bar{5}}{}' = 4.4 \pm 0.3$				
3	6	$\bar{6}$	3	$\pi_{3\bar{6}}{}' = (\pi_{31} + \pi_{32})/2 = 1.8 \pm 0.5 \quad (2.8)^b$	$\pi_{66} = -9.7 \pm 0.9$	$\pi_{66} = -10.4 \pm 1.7$	$\pi_{6\bar{6}}{}^* = \pi_{\bar{6}\bar{6}}{}'{n_6}^3 - \pi_{3\bar{6}}{}'{n_3}^3 = -18.5$	$\pi_{6\bar{6}}{}^* = -16.5 \pm 0.7$
	6	$\bar{6}$	$\bar{6}$	$\pi_{\bar{6}\bar{6}}{}' = (\pi_{11} + \pi_{12} + \pi_{21} + \pi_{22} + 2\pi_{66})/4 = 2.6 \pm 0.4$				
3a	$\bar{6}$	6	3	$\pi_{36}{}' \equiv \pi_{3\bar{6}}{}' = 4.0 \pm 0.8 \quad (2.8)^b$	$\pi_{66} = -11.1 \pm 0.9$	$\pi_{66} = -10.4 \pm 1.7$	$\pi_{\bar{6}\bar{6}}{}^* = \pi_{66}{}'{n_6}^3 - \pi_{36}{}'{n_3}^3 = -9.3$	$\pi_{\bar{6}\bar{6}}{}^* = -14.6 \pm 0.6$
	$\bar{6}$	6	6	$\pi_{66}{}' \equiv \pi_{\bar{6}\bar{6}}{}' = 2.0 \pm 0.4$				

[a]All values are in units of Br ($=10^{-12}$ m^2/N). The mechanical compression is parallel to the [110], [101], or [011] direction.
[b]Effective values calculated from the data presented in Table 1.

Table 3. Calculated Photoelastic Constants p_{ef} and Figure of Merit M_2 for Cs_2HgCl_4 Crystals[a]

Type of Acousto-optical Diffraction	Polarization of Optical Wave		Acoustic Wave			Effective Coefficient $p_{ef} = p_{in}$	$M \times 10^{15}$ (s^3/kg)	$M \times 10^{15}$ for α-HIO_3 (s^3/kg)
	Incident Light	Diffracted Light	Propagation Polarization	Mode[b]	Velocity $V \times 10^{-3}$ (m/s)			
Isotropic	[100]	[100]	[100]	L	2.51	$p_{11} = 0.40$	50	48
Isotropic	[100]	[100]	[010]	L	1.91	$p_{12} = 0.40$	114	42
Isotropic	[100]	[100]	[001]	L	1.96	$p_{13} = 0.39$	100	83
Isotropic	[010]	[010]	[100]	L	2.51	$p_{21} = 0.26$	23	21
Isotropic	[010]	[010]	[010]	L	1.91	$p_{22} = 0.29$	65	58
Isotropic	[010]	[010]	[001]	L	1.96	$p_{23} = 0.34$	85	78
Isotropic	[001]	[001]	[100]	L	2.51	$p_{31} = 0.17$	9.0	46
Isotropic	[001]	[001]	[010]	L	1.91	$p_{32} = 0.19$	26	33
Isotropic	[001]	[001]	[001]	L	1.96	$p_{33} = 0.25$	41	63
Anisotropic	[010]	[001]	[010], [001]	T	0.87	$p_{44} = -0.034$	7.1	18
Anisotropic	[100]	[001]	[100], [001]	T	1.06	$p_{55} = -0.026$	3.8	25
Anisotropic	[100]	[010]	[100], [010]	T	0.87	$p_{66} = -0.032$	7.0	28

[a]The figure of merit is calculated only for the principal crystallographic directions.
[b]L, T, the longitudinal and the transverse acoustic waves, respectively.

lated directly from the effective piezo-optical constants π_{44}', π_{55}', and π_{66}' and $\pi_{\bar{4}\bar{4}}'$, $\pi_{\bar{5}\bar{5}}'$, and $\pi_{\bar{6}\bar{6}}'$ measured by one-stage and two-stage methods.

3. Photoelastic Constants P_{in} and Figure of Merit M_2

We calculated the photoelastic constants p_{in} of Cs_2HgCl_4 crystals ($p_{in} = \pi_{im}C_{mn}$), using the data of Tables 1 and 2 and the elastic constants C_{mn} from Ref. 7. These constants are presented in Table 3. It must be noted that the photoelastic effect in these crystals is stronger than in well-known acousto-optical materials such as TeO_2 and $PbMoO_4$, for which the largest photoelastic constants are $p_{13} = 0.34$ and $p_{33} = 0.30$,[12] respectively. It is more interesting, however, to compare their acousto-optical properties. Figure of merit M_2 is one of the most important parameters that characterize the acousto-optical interaction[12] (a comprehensive description is given also in Refs. 13 and 14). Table 3 lists the magnitudes of M_2 for Cs_2HgCl_4 crystals that were calculated for the principal crystallographic directions according to the formula

$$M_2 = p_{ef}^2 \tilde{n}^6/\rho V^3, \quad (4)$$

where we consider $\tilde{n}^6 \approx (n_i n_d)^3$ ($\tilde{n}$ is the average refractivity; n_i and n_d are the refractive indices of the incident and the diffracted light, respectively), ρ is the crystal density, V is the ultrasonic wave velocity and p_{ef} is the effective photoelastic constant. For comparison, the data for the well-known acousto-optical material α-HJO_3 (Refs. 15 and 16) are presented in Table 3 as well. It is surprising that both of these crystals have the same orthorhombic symmetry and are water soluble. A strong photoelastic effect and low ultrasonic velocities in Cs_2HgCl_4 [for comparison, the longitudinal acoustic L modes in α-HJO_3 *have the following velocities:* $V_{11} = 3560$ m/s and $V_{22} = 2890$ m/s (Ref. 14)] represent a substantial figure of merit (i.e., high diffraction efficiency) compared with that of α-HJO_3 crystals in the case of the isotropic diffraction. The priority for Cs_2HgCl_4 crystals is the acousto-optical interaction between the acoustic L modes V_{22} *or* V_{33} and an optical wave polarized along [100] (Table 3). Those interactions are characterized by the figures of merit $M_2 = 114 \times 10^{-15}$ s^3/kg and $M_2 = 100 \times 10^{-15}$ s^3/kg, respectively. For comparison, the largest diffraction efficiency in α-HJO_3 ($M_2 = 83 \times 10^{-15}$ s^3/kg) appears in the isotropic acousto-optical interaction between the acoustic L mode V_{33} and the optical wave polarized along [100].

Unfortunately, figure of merit M_2 is not so substantial for anisotropic diffraction, as one can see for the several geometries of the acousto-optical interaction presented in Table 3. However, we do not exclude the possibility of larger diffraction efficiency in Cs_2HgCl_4 crystals when the optical and acoustic waves propagate along nonprincipal crystallographic directions. In this respect a more-detailed analysis would be quite useful, but it is beyond the scope of this paper.

The advantage of Cs_2HgCl_4 crystals compared with other acousto-optical materials is the anisotropy of their acoustical and optical properties, which permits the choice of an optimal combination for the design of acousto-optical devices. In particular, Cs_2HgCl_4 are optically biaxial crystals. Hence they can be considered promising materials for the design of acousto-optical cells with low optical losses, which may be achieved with sample geometries with a wide range of acousto-optical interaction angles.[12] The list of materials of a similar type with good acousto-optical properties seems not to be long. Another important characteristic of this type of crystal is acoustic walk-off (or obliquity) angle θ. Figure 1 shows the dependence of walk-off angle θ on the direction of sound propagation calculated in way similar to that in Ref. 17 in the principal crystallographic *XY*, *XZ*, and YZ planes. The maximum angles θ appear in the *XY* plane. Their magnitudes are similar to the obliquity

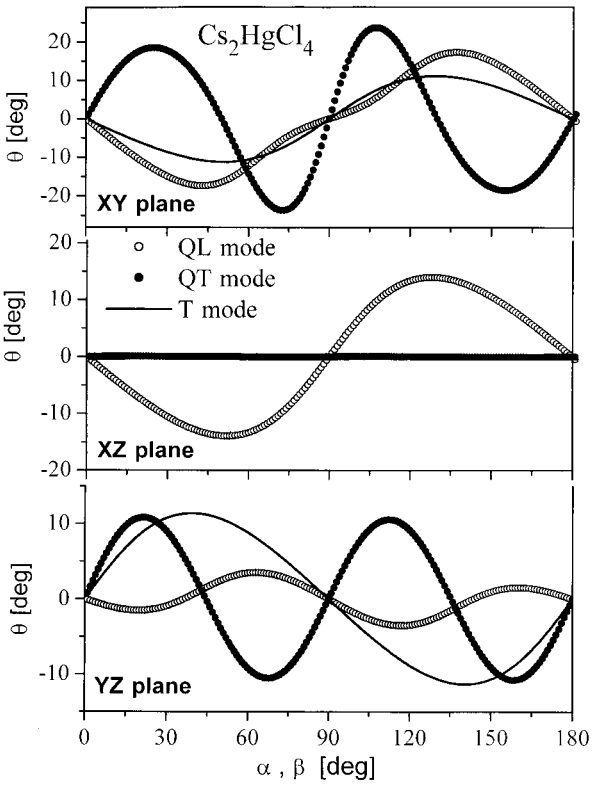

Fig. 1. Dependence of acoustic walk-off angle θ on direction of sound propagation in the principal crystallographic *Xy*, *XZ*, and *YZ* planes of Cs_2HgCl_4 crystals.

angles that can be observed in isostructural compounds Cs_2CdBr_4 and Cs_2HgBr_4.[17] The plots for the *XZ* and *YZ* planes are peculiar. The acoustic walk-off angle for the quasi-longitudinal *Q*L mode (*YZ* plane) increases slightly, reaching its maximum value of ~4° at an angle $\beta = 63°$ to the *Y* axis. One can see that the obliquity angles for quasi-transverse (*QT*) and purely transverse *T* modes do not exceed $\theta = 1°$ for any arbitrary direction in the *XZ* plane. This fact is not unusual: There is only a weak anisotropy of phase velocities for *Q*T and *T* modes in this plane. The acoustic walk-off angle always passes through its zero value ($\theta = 0$) at $\alpha, \beta, \gamma = 90$ n ($n = 0, 1, 2 \ldots$) in accordance with the requirements of the crystal symmetry.

4. Conclusion

In conclusion, we have presented the results of our piezo-optical investigations of Cs_2HgCl_4 crystals at room temperature. All the components of piezo-optical tensor π_{mn} and photoelastic tensor p_{in} were obtained. The substantial photoelastic effect and low ultrasonic velocities cause a relatively high figure of merit M_2 for the isotropic diffraction (for a certain geometries of the piezo-optical interactions, $M_2 \sim 110 \times 10^{-15}$ s^3/kg). Cesium mercury tetrachlorate can be considered, therefore, a new material for acousto-optical applications. The dependence of the acoustic walk-off angle on the direction of sound propagation in the principal crystallographic planes has been calculated.

References

1. B. Sh. Bagautdinov, I. D. Brown, Yu. I. Yuzuyk, and V. P. Dmitriev, "X-ray diffraction study of a sequence of phase transitions in Cs_2HgCl_4 crystals," Phys. Solid State **43,** 350–354 (2001).
2. V. P. Dmitriev, Yu. I. Yusyuk, A. V. Tregubchenko, E. S. Larin, V. V. Kirilenko, and V. I. Pakhomov, "Phase sequence and lattice dynamics in Cs_2HgCl_4," Sov. Phys. Solid State **30,** 704–706 (1988).
3. S. N. Kallayev, V. V. Gladkii, V. A. Kirikov, and I. K. Kamilov, "Phase transitions in Cs_2HgCl_4 crystals," Ferroelectrics **106,** 299–302 (1990).
4. V. V. Petrov, A. Yu. Halahan, V. G. Pitsyuga, and V. E. Yachmenov, "Low-temperature specific heat in Cs_2HgCl_4 and Cs_2HgBr_4 crystals," Sov. Phys. Solid State **30,** 906–908 (1988).
5. A. V. Kityk, O. M. Mokry, V. P. Soprunyuk, and O. G. Vlokh, "Optical birefringence and acoustical properties near the phase transitions and triple point in incommensurate proper ferroelastic Cs_2HgBr_4, Cs_2CdBr_4 and Cs_2HgCl_4 crystals," J. Phys. Condens. Matter **5,** 5189–5200 (1993).
6. A. V. Kityk, Ya. I. Shchur, A. V. Zadorozhna, I. B. Trach, I. S. Girnyk, I. Yu. Martynyuk-Lototska, and O. G. Vlokh, "Pressure induced ferroelastic instability and lattice dynamics of Cs_2HgCl_4 crystals within the semiempirical rigid-ion model," Phys. Rev. B **58,** 2505–2512 (1998).
7. A. V. Kityk, A. V. Zadorozhna, Ya. I. Shchur, I. Yu. Martynyuk-Lototska, and O. G. Vlokh, "Lattice instability of Cs_2HgCl_4 crystals. I. Elastic properties," Phys. Status Solidi B **210,** 35–45 (1998).
8. A. V. Kityk, Institute for Computer Science, Technical University of Czestocowa, PL-42200 Czestocowa, Poland, and A. V. Zadorozhna are preparing a manuscript to be called "Optical refraction and absorption of Cs_2HgCl_4 crystals."
9. B. G. Mytsyk, Ya. V. Pryriz, and A. S. Andrushchak, "the lithium niobate piezooptical features," Cryst. Res. Technol. **26,** 931–940 (1991).
10. N. A. Romanyuk, B. G. Mytsyk, and L. N Kulyk, "Piezoizmenenija opticheskikh svojstv kristallov triglicynsulfata," Ukr. Fiz. Zh. **31,** 354–359 (1986).
11. T. S. Narasimhamurty, *Photoelastic and Electro-Optic Properties of Crystals* (Osmania U Press, Hyderabad, India; Plenum, New York, 1981).
12. B. I. Balakshyj, V. N. Parygin, and L. E. Chirkov, *Fizicheskie Osnovy Akusto-Optiki* (Radio i Svjaz, Moscow, 1985).
13. A. Korpel, *Acousto Optics*, 2nd ed. (Marcel Dekker, New York, 1996).
14. J. Xu and R. Stround, *Acousto-Optic Devices: Principles, Design, and Applications* (Wiley, New York, 1992).
15. I. M. Silvestrova, N. S. Spiridonova, N. A. Moisejeva, and Yu. V. Pisarevskij, "Acoustooptical properties of α-HJO_3 crystals," preprint 365 (Institute for Crystallography Academy of Science USSR, Moscow, 1991).
16. D. A. Pinnow and R. W. Dixon, "Alpha-iodic acid: a solution-grown crystal with a high figure of merit for acousto-optic device applications," Appl. Phys. Lett. **13,** 156–158 (1968).
17. A. V. Kityk, A. V. Zadorozhna, Ya. I. Shchur, I. Yu. Martynyuk-Lototska, Ya. Burak, and O. G. Vlokh, "Elastic properties of Cs_2HgBr_4 and Cs_2CdBr_4 crystals," Austral. J. Phys. **51,** 643–657 (1998).